

AperTO - Archivio Istituzionale Open Access dell'Università di Torino

**Tuning the Activity and Selectivity of CuCl<sub>2</sub>/gamma-Al<sub>2</sub>O<sub>3</sub> Ethene Oxychlorination Catalyst by Selective Promotion**

**This is the author's manuscript**

*Original Citation:*

*Availability:*

This version is available <http://hdl.handle.net/2318/152489> since 2016-10-08T16:19:33Z

*Published version:*

DOI:10.1007/s11244-013-0231-y

*Terms of use:*

Open Access

Anyone can freely access the full text of works made available as "Open Access". Works made available under a Creative Commons license can be used according to the terms and conditions of said license. Use of all other works requires consent of the right holder (author or publisher) if not exempted from copyright protection by the applicable law.

(Article begins on next page)



# UNIVERSITÀ DEGLI STUDI DI TORINO

*This is an author version of the contribution published on:*

*Questa è la versione dell'autore dell'opera:*

## **Tuning the activity and selectivity of $\text{CuCl}_2/\gamma\text{-Al}_2\text{O}_3$ ethene oxychlorination catalyst by selective promotion**

by

Naresh B. Muddada, Terje Fuglerud, Carlo Lamberti, Umni Olsbye

*Top. Catal.* **57** (2014) 741-756.

doi: 10.1007/s11244-013-0231-y

***The definitive version is available at:***

*La versione definitiva è disponibile alla URL:*

<http://link.springer.com/article/10.1007%2Fs11244-013-0231-y>

# Tuning the activity and selectivity of $\text{CuCl}_2/\gamma\text{-Al}_2\text{O}_3$ ethene oxychlorination catalyst by selective promotion

Naresh B. Muddada<sup>1</sup>, Terje Fuglerud<sup>2</sup>, Carlo Lamberti<sup>3</sup>, Unni Olsbye<sup>1\*</sup>

<sup>1</sup> inGAP Centre of Research-based Innovation, Department of Chemistry, University of Oslo, Sem Sælandsvei 26, N-0315 Oslo, Norway.

<sup>2</sup> Technology and Projects, INEOS ChlorVinyls, Herøya Industrial Park, N-3936, Porsgrunn, Norway.

<sup>3</sup> Department of Inorganic, Physical and Materials Chemistry and NIS Centre of Excellence, Università di Torino, Via P. Giuria 7, 10125 Torino, Italy.

## Abstract

$\text{CuCl}_2/\gamma\text{-Al}_2\text{O}_3$  catalysts with and without promoter metal chlorides (Cu5.0, K3.1Cu5.0, La10.9Cu5.0, Li0.5Cu5.0, Cs10.4Cu5.0, Mg1.9Cu5.0, Ce5.5La5.45Cu5.0, and K1.55La5.45Cu5.0) were studied for the ethene oxychlorination reaction in a fixed-bed reactor at 503 and 573 K, with  $\text{C}_2\text{H}_4 : \text{HCl} : \text{O}_2 : \text{He} = 1.0 : 1.1 : 0.38 : 14.4$  (mole ratio),  $P(\text{tot}) = 1$  atm and  $\text{WHSV} = 1.5$  g/g\*hr (based on ethene). It was found that all promoter metals enhanced the activity of the catalyst, as well as its selectivity towards the target product 1,2-dichloroethane (1,2-EDC). Co-promoted catalysts (K1.55La5.45Cu5.0 and Ce5.5La5.45Cu5.0) gave even higher activity and product selectivity than the single metal promoted catalysts.

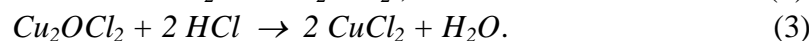
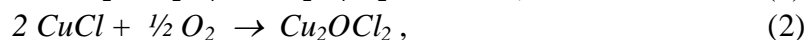
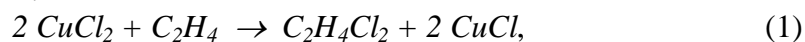
The activity of the  $\text{CuCl}_2/\gamma\text{-Al}_2\text{O}_3$  catalyst, as well as the  $\gamma\text{-Al}_2\text{O}_3$  support, both with and without metal chloride promoter(s), were further tested for 1,2-EDC conversion to byproducts in a fixed-bed reactor at 503 K, under a feed stream of 1,2-EDC: Ar = 1 : 11.5 (mole ratio), at  $P(\text{tot}) = 1$  atm and  $\text{WHSV} = 1.5$  g/g\*hr (based on 1,2-EDC). Prior to testing, the catalysts were pretreated in flowing ethene, HCl and/or  $\text{O}_2$ . It was observed that Lewis and Brønsted acid sites on the alumina surface were main reaction sites for conversion of 1,2-EDC to chlorinated byproducts (vinyl chloride monomer (VCM), 1,1-EDC, 1,2-dichloroethene (1,2-DCE) and ethyl chloride (EC)) as well as dimerisation (butadiene) and aromatisation reactions (toluene), both with and without the presence of the Cu phase. The Cu phase was shown to contribute mainly to  $\text{CO}_2$  and trichloroethane (TCE) formation from 1,2-EDC via VCM route. Co-promotion (K1.55La5.45Cu5.0) was found to enhance the activity of the Cu phase, and to mask acid sites on the alumina surface, thereby promoting ethene oxychlorination while at the same time hindering undesired conversion of the target product 1,2-EDC.

## 1. Introduction

Fine-tuning of the catalyst surface, in combination with a detailed fundamental understanding of the reaction mechanism, is an important research topic of industrial catalysis in the 21<sup>st</sup> century<sup>1</sup>. Oxychlorination of ethene to 1,2-dichloroethane (1,2-EDC) is a crucial step<sup>2</sup> in the production of PVC (Poly-Vinyl Chloride), a versatile plastic material. PVC is obtained by the polymerization of vinyl chloride monomer (VCM)<sup>2a</sup> which is produced by cracking of 1,2-dichloroethane (EDC). The process is illustrated in Scheme 1.

The oxychlorination step is catalyzed by  $\text{CuCl}_2$  supported on  $\gamma$ -alumina at 490-573 K and 5-6 atm using either air or oxygen in fluid or fixed bed reactors<sup>2a</sup> via a three step reaction

mechanism<sup>15a-b,14b</sup> as shown in Eqs (1) to (3). Commercial catalysts are produced by impregnation of the support with  $\text{CuCl}_2$  solution, and contain various promoter metal chlorides<sup>1,3</sup> (mainly alkali, alkaline earth or rare earth metal chlorides) in variable concentration<sup>2a</sup>.



Despite the use of promoters and the high state of development of the process, a considerable amount of  $\text{C}_1, \text{C}_2$ -poly unsaturated chloro-hydrocarbons is formed at rates that depend on various factors such as temperature, the state of the catalyst surface and feed composition<sup>2a,4</sup>. Especially, as temperature increases, the product distribution changes from high yields of 1,2-dichloroethane (1,2-EDC) towards a mixture of chlorinated hydrocarbons, including vinyl chloride ( $\text{C}_2\text{H}_3\text{Cl}$ ; VCM), 1,1,2-trichloroethane ( $\text{C}_2\text{H}_3\text{Cl}_3$ ; TCE), ethylchloride ( $\text{C}_2\text{H}_5\text{Cl}$ ; EC), trichloroethene ( $\text{C}_2\text{HCl}_3$ ), 1,1-dichloroethane ( $\text{C}_2\text{H}_4\text{Cl}_2$ ; 1,1-EDC), 1,2-dichloroethene ( $\text{C}_2\text{H}_2\text{Cl}_2$ ; DCE), carbon tetrachloride ( $\text{CCl}_4$ ; CTC), methyl chloride ( $\text{CH}_3\text{Cl}$ ; MC) and 1,1,2,2-tetrachloroethane ( $\text{C}_2\text{H}_2\text{Cl}_4$ ), as well as  $\text{CO}_x$ . Though the present industrial reactors are generally operating at 1,2-EDC selectivities higher than 95 %, the abundance of this process makes further improvement of its selectivity an important target, both from an environmental and economic perspective.

Literature studies<sup>4a,b,5</sup> suggest that chlorinated byproducts are formed by the subsequent reactions of 1,2-EDC, while  $\text{CO}_x$  formation results from oxidation of the starting materials. All these reactions are believed to be catalytic<sup>5a,b,6</sup>, since, the non-catalytic (gas-phase) dehalogenation or oxidation reactions of haloalkanes have high activation energies and therefore demand high reaction temperatures<sup>7</sup>. Several authors<sup>5-6,8</sup> contributed to the current understanding of by-product formation. Finocchio *et al*<sup>8a</sup> investigated the un-promoted  $\text{CuCl}_2$  system and suggested that uncovered alumina surface plays a negative role, by catalysing the dehydrochlorination of 1,2-EDC to VCM in the oxychlorination reactor. Subsequently, VCM would produce the main by-product TCE. Shalygin *et al*<sup>8b</sup> studied the activity of 1,2-EDC on  $\gamma$ - alumina support at 673 K using IR spectroscopy and suggested that dehydrochlorination of 1,2-EDC to VCM occurred on Lewis acid sites on the surface, which is in line with observations made by other authors<sup>5a,6a,8c,d,9</sup>.

Mile *et al*<sup>8c</sup> studied 1,2-dichloroethane conversion over copper chloride supported on alumina in the temperature range 473-623 K using a micro reactor, and reported plots of  $\ln[\text{vol } 1,2\text{-EDC in} / \text{vol } 1,2\text{-EDC out}]$  versus residence time (0.2 s to 1.0 s) at different temperatures. From the experimental observations, the authors concluded that the primary dehydrochlorination reaction of 1,2-EDC is a first order reaction with a rate constant  $k_{\text{EDC}} = 0.168 \text{ s}^{-1}$  and an activation energy of 103 kJ/mol at 558 K. The authors further reported that addition of promoter metal chlorides decreased the rate constant  $k_{\text{EDC}}$  in the following order  $\text{LiCl} > \text{CsCl} > \text{NaCl} > \text{KCl} \sim \text{RbCl}$ , mainly due to an increase in the respective activation energies<sup>8c</sup>. From isotope labeling experiments, a primary kinetic isotope effect  $k_{\text{EDC}}/k_{\text{deutero-EDC}}$  of 1.87 was observed at 558 K for perdeuterated 1,2-dichloroethane. The authors suggested that C-H bond breaking occurred as the rate determining step. They further suggested that the Lewis acid character of  $\text{CuCl}_2$  could assist the C-Cl bond rupture and the formation of a carbonium ion, while the intermediate  $\text{Cu}_2\text{OCl}_2$  could act as a basic site for C-H bond cleavage and carbanion formation.

Members of our team have studied the ethene oxychlorination reaction over Cu-based catalysts for more than a decade. The present work is an extension of our previous works<sup>10</sup>;

where we studied the effect of promoters (KCl, CsCl, LiCl, MgCl<sub>2</sub>, CeCl<sub>3</sub>, and LaCl<sub>3</sub>) on the nature, relative fraction, dispersion, and reducibility of copper chloride species on CuCl<sub>2</sub>/M/ $\gamma$ -Al<sub>2</sub>O<sub>3</sub> oxychlorination catalysts (M = promoter). The following conclusions were drawn:

1. CuCl<sub>2</sub>, when impregnated on  $\gamma$ -Al<sub>2</sub>O<sub>3</sub>, forms two phases, one Cu-aluminate phase (0.95 wt% Cu forms as Cu-aluminate per 100 m<sup>2</sup>/g surface area of alumina) and the rest as a Cu-chloride phase. The various copper phases were detected by using complementary techniques, such as UV-vis spectroscopy, EXAFS and EPR spectroscopy<sup>10b,15a</sup>.
2. In-situ EXAFS studies showed that the addition of promoters (LaCl<sub>3</sub>, MgCl<sub>2</sub>, LiCl, KCl and CsCl) to the CuCl<sub>2</sub>/ $\gamma$ -Al<sub>2</sub>O<sub>3</sub> catalyst increased the fraction of Cu<sup>2+</sup> in the chloride form<sup>10c</sup>. All promoter cations compete with copper ions to occupy the octahedral vacancy sites of  $\gamma$  - alumina support with the following trend: K<sup>+</sup>  $\leq$  Cs<sup>+</sup>  $\leq$  Li<sup>+</sup>  $\ll$  Mg<sup>2+</sup>  $<$  La<sup>3+</sup>. Furthermore, some promoters enhanced the Cu dispersion, in the order: LiCl  $>$  LaCl<sub>3</sub>  $>$  MgCl<sub>2</sub>. Conversely, KCl and CsCl addition decreased the Cu-dispersion<sup>10c</sup>.
3. Infrared spectroscopy of adsorbed CO at liquid nitrogen temperature on  $\gamma$ -Al<sub>2</sub>O<sub>3</sub> promoted with LaCl<sub>3</sub>, MgCl<sub>2</sub>, LiCl, KCl and CsCl showed that CsCl and KCl promotion eliminated the surface Lewis acidity, while all other tested promoters strongly suppressed it. An increase in the strength of the Brønsted acid sites was observed in all cases except for CsCl promotion<sup>10b</sup>.
4. In all these promoted catalysts, a positive trend was found between the density of Lewis acid sites and byproduct selectivity in the ethene oxychlorination reaction at 503 - 573 K. Furthermore, there was a positive correlation between the density of Lewis acid sites and the  $\pi$  back donation capability of Cu(I) species. Surprisingly, the density and strength of Brønsted acid sites had no straightforward correlation with byproduct formation<sup>10b</sup>.
5. Operando XANES studies<sup>10a</sup> performed on the catalysts (as such and promoted) under steady state ethene oxychlorination conditions (C<sub>2</sub>H<sub>4</sub>: HCl: O<sub>2</sub>: N<sub>2</sub> = 100 : 36.1 : 7.6 : 180 Nml/min) in the temperature range 373 – 623 K showed that addition of K and Cs chlorides increased the relative fraction of Cu(II) vs. Cu(I) on the surface compared to rest of the catalysts. It is believed that K and Li promotion slow down the first step in the oxychlorination cycle (Eq. (1)), thus rendering the catalyst predominantly in the oxidized state: Cu (II)<sup>10d,a</sup>.
6. After careful evaluation of the results from several complimentary techniques<sup>10a-c</sup> (UV, IR, EXAFS, CO-chemisorption and reaction studies), it was suggested that the change in Cu oxidation state could be due to the formation of mixed chloride phases, notably CuK<sub>x</sub>Cl<sub>x+2</sub> and CuCs<sub>x</sub>Cl<sub>2+x</sub>.

Based on the available literature data<sup>5b,c,6a,8b-d</sup> and from our experience<sup>10</sup>, it is believed that there might be five possible active sites for further conversion of 1,2-dichloroethane on CuCl<sub>2</sub>/ $\gamma$ -Al<sub>2</sub>O<sub>3</sub> catalyst during the oxychlorination reaction, leading to the formation of a variety of by-products. For the bare catalyst, the five possible active sites are CuCl<sub>2</sub>, Cu<sub>2</sub>OCl<sub>2</sub>, CuCl, Lewis acid sites [Al<sup>3+</sup>] and Brønsted acid sites [Al-OH] on the catalyst surface. For promoted catalysts, the respective promoter metals may also act as active sites.

In the current contribution, our aim is to decouple the effects of support, promoter and Cu oxidation state on the formation of byproducts during the oxychlorination reaction. For this purpose, Cu/ $\gamma$ -Al<sub>2</sub>O<sub>3</sub> catalyst was impregnated with a range of promoters (LaCl<sub>3</sub>, MgCl<sub>2</sub>, LiCl, KCl, CsCl, CeO<sub>2</sub>+LaCl<sub>3</sub> and KCl+LaCl<sub>3</sub>) while  $\gamma$ -Al<sub>2</sub>O<sub>3</sub> support was impregnated with KCl, LaCl<sub>3</sub>, and KCl+LaCl<sub>3</sub>. The Cu-containing samples were subjected to catalytic testing

for the ethene oxychlorination reaction in a fixed bed reactor at 503 and 573 K. Furthermore, the support and catalyst samples with and without KCl, LaCl<sub>3</sub>, and KCl+LaCl<sub>3</sub> promoters were subjected to testing for 1,2-EDC conversion in a fixed bed reactor at 503 K. Before feeding 1,2-EDC, the state of the Cu phase was in each case altered by in-situ pretreatment under flowing ethene, O<sub>2</sub>, and/or HCl (cfr Eq. (1) to (3) above).

## 2. Experimental methods

### 2.1. Sample Preparation

All samples were prepared by impregnation of  $\gamma$ -alumina (Condea Puralox SCCa 30/170, surface area: 168 m<sup>2</sup> g<sup>-1</sup>, pore volume: 0.50 cm<sup>3</sup> g<sup>-1</sup>) with aqueous solutions of the corresponding chlorides following the incipient wetness method<sup>10a,b,11</sup>. After impregnation, catalysts were dried at 393 K under a dry air-flow for 3 h and then kept at room temperature. All samples were labeled according to wt.% content of the different metals (Cu and promoter). As an example, sample Cu5.0 represents a 5.0 wt.% Cu loaded sample without additives, while sample K3.1Cu5.0 represents a catalyst prepared with 5.0 wt.% Cu plus 3.1 wt.% K impregnated in the chlorinated form (KCl). In all catalysts, the amount of copper was fixed to 5 wt.%, while for the promoted samples, the molar fraction between Cu and the promoter(s) was 1:1, resulting in Li0.5Cu5.0, K3.1Cu5.0, Cs10.4Cu5.0, Mg1.9Cu5.0, Ca3.2Cu5.0, La10.9Cu5.0, Ce5.5La5.45Cu5.0 and K1.55La5.45Cu5.0 catalysts. To elucidate the effect of the bare support and promoter metal alone, three samples of promoted supports were prepared by the same method and promoter amounts as used for the preparation of catalysts, i.e., K3.1A, La10.9A, and K1.55La5.45A supports (A= bare alumina support).

### 2.2. Fixed-bed catalytic activity tests

All catalytic tests were performed in a fixed-bed quartz reactor (10 mm inner diameter). The reaction temperature was measured by a thermocouple in a quartz thermocouple well with outer diameter 3 mm, which was centered axially in the reactor. All feed lines were made of Teflon.

#### 2.2.1 Ethene oxychlorination

Catalytic tests for the ethene oxychlorination reaction were performed at 503 and 573 K. The catalyst (0.2 g, 250–450  $\mu$ m) was diluted with graphite (0.4 g, 250–450  $\mu$ m). In all experiments, the catalyst was activated in-situ at 503 K for 1 h under Ar gas flow, before exposing it to the reactant mixtures. The molar feed gas composition was C<sub>2</sub>H<sub>4</sub>: HCl: O<sub>2</sub>: He = 1: 1.10: 0.38: 14.4 with total feed rate of 45 Nml/min, P<sub>(tot)</sub> = 1 atm and WHSV = 1.5 g/g\*hr (based on ethene). The contents of the light gases (C<sub>2</sub>H<sub>4</sub>, O<sub>2</sub> and N<sub>2</sub>) in the effluent stream were determined by an on-line HP 5973 GC equipped with column-switching valves and TCD (thermal conductivity detector) following a separation in Plot Q and molecular sieve columns operated at 573 K. The chlorinated products in the effluent stream were analyzed using an off-line HP6950 GC-MS equipped with DB-1 column, coupled with a quadruple mass spectrometer. GC and GC-MS analysis were made after 60 min of isothermal reaction. Reaction selectivity towards chlorinated by-products was estimated by dividing the (respective product area\*100) by the total area of the products including 1,2-EDC (1,2-dichloroethane).

#### 2.2.2 1,2-EDC conversion

The catalytic activity in the conversion of 1,2-EDC was measured at 503 K and P<sub>(tot)</sub> = 1 atm with WHSV of 1.5 g of 1,2-EDC\*g cat<sup>-1</sup>\* h<sup>-1</sup>. The molar feed gas composition was 1,2-EDC : Ar = 1 : 11.5. The reactor was loaded with 0.5 g of the catalyst (250-450  $\mu$ m) and 0.1 g of graphite granules (250-450  $\mu$ m). The temperature of the catalyst bed was controlled within an error of  $\pm 1$  °C. The reaction of 1,2-EDC was operated in the kinetic regime with

low conversions ranging from 0-5%. The effluent stream was further diluted with helium, in order to avoid corrosion and condensation problems in downstream analytical equipment. The diluted effluent stream was analyzed with an on-line Quadruple Mass Spectrometer. Chlorinated products in the effluent stream were further analyzed using on-line GC-MS (Agilent HP 6950) equipped with DB-1 column and quadruple mass spectrometer. Intensities of reactants and products were further normalized using argon as reference gas. At each step of 1,2-EDC interaction (see below), on-line sampling were made to GC-MS after 15 and 55 min on stream.

Experimental procedure. In first set of experiments, 1,2-EDC conversion was performed on the support samples, in order to elucidate the activity of the alumina support and the influence of the promoter metal. In such experiments, after thermal activation of the samples at 503 K for 1 h under Ar gas flow, 1,2-EDC feed stream was sent over the reactor for 2 h with simultaneous analysis of the effluent stream. After 2 h of 1,2-EDC interaction, the reactor was purged with Ar for 15 min, followed by interaction with HCl+Ar gas feed stream for 30 min. Then the system was again purged with Ar, to flush off all the physisorbed HCl on the feed lines, reactor walls and catalyst surface. After purging for 15 min, 1,2-EDC feed stream was again sent over the reactor for 1 h.

In the second set of experiments, 1,2-EDC conversion experiments were performed on the catalyst samples, in order to elucidate the activity of the copper chloride species and the influence of the promoter metal. In such experiments, a systematic study of reactant gas and 1,2-EDC feed stream was adopted. The thermally activated catalyst was first interacted with each reactant in a step wise manner (Eqs.1-3), while purging with Ar between each cycle. The main purpose of this procedure was to pre-activate of the copper (II) chloride sites on the surface of the catalyst before interaction with 1,2-EDC. The experimental procedure is illustrated in Fig. 1, which shows the MS response of the effluent gases. At  $t_1$ ,  $C_2H_4$  flow was introduced to the reactor to modify the catalyst surface to contain mainly  $Cu(I)Cl$  species (Eq. (1)). After 30 min on stream, at  $t_2$ ,  $C_2H_4$  was switched off and the system purged with Ar gas for 15 min. 1,2-EDC feed was switched on at  $t_3$  and kept under constant flow for 1 h. Products in the effluent stream were analyzed by MS and also by GC-MS during this cycle. At  $t_4$ , 1,2-EDC flow was switched off and the system purged with Ar gas flow for 15 min. Then at  $t_5$ , air flow was introduced to oxidize all cuprous species and modify the catalyst surface to contain mainly  $Cu_2OCl_2$  species (Eq. (2)), followed by Ar purging. At  $t_6$ , 1,2-EDC flow was switched on and kept under constant flow for 1h followed by sampling. At  $t_7$  and  $t_8$ , Ar purging and HCl flow were switched on, respectively, to regenerate the catalyst surface to the  $CuCl_2$  state (Eq. (3)). Please note that, during HCl feeding in the reported experiment, i.e. between the time  $t_9 - t_{10}$ , the MS was by-passed, owing to its sensitivity to corrosion. Instead, the MS signal acquired during a previous test with HCl – catalyst interaction is shown in the inset in Fig. 1. The 1,2-EDC flow was switched on at  $t_{10}$ , and kept constant for 1h, whereupon products were analyzed by GC-MS.

Although the system was purged with Ar between each reaction step, it is expected that traces of hydrogen chloride and 1,2-dichloroethane will be left on the sample and on the reactor walls. Minor  $CO_2$  peaks were observed in all tests reported in this work. However, when the amount of  $CO_2$  did not exceed that observed in blank tests performed by feeding an empty reactor with Ar gas, it was not considered a reaction product.

### 3. Results

#### 3.1. Influence of Cu, promoter metals and chlorine species on the acidity of $\gamma$ -alumina surface

It has been suggested that some by-product formation reactions were catalyzed by the acidic sites on the alumina support<sup>5-6,8a-c</sup>. In the following, we will therefore provide a brief summary of a previously published FTIR study of the supports and catalysts used in this work<sup>10b</sup>. As far as  $\gamma$ -alumina is concerned, the oxide surface is considered to contain three different types of sites: the  $O^-$  anions can act as electron-donating Lewis base sites and incompletely coordinated  $Al^{3+}$  as electron-accepting Lewis acid sites, while the  $>Al-OH$  are Brønsted acid sites<sup>12</sup>.

The IR spectra of CO dosed at liquid nitrogen temperature on the supports ( $\gamma-Al_2O_3$ , La10.9A, K3.1A), on the chlorinated supports (Cl1.4A, Cl2.8A), and on the catalysts (Cu5.0, La10.9Cu5.0, K3.1Cu5.0), are reported in Fig. 2 **Error! Reference source not found.** All the samples were pre-activated at 503 K for 1 hr in dynamic vacuum. The interaction between CO and surface sites can be separated into an electrostatic, a covalent  $\sigma$ -dative and a  $\pi$ -back donation contribution, the first two causing a blue shift of the  $\nu(CO)$ , while the last causes a red shift<sup>10b,13</sup>, with respect to the unperturbed molecule:  $\nu_0(CO) = 2143\text{ cm}^{-1}$ . On the surface of pure alumina, CO interacts with both Brønsted and Lewis sites; the latter one will be observed only when the experiments are performed at liquid nitrogen temperature. A blue shift  $\Delta\nu(CO) = \nu(CO) - \nu_0(CO) > 0$ , is expected in both cases, where usually the  $\nu(CO)$  in the  $2230-2180\text{ cm}^{-1}$  and in  $2160-2175\text{ cm}^{-1}$  ranges for  $Al^{3+}\cdots CO$  and  $Al-OH\cdots CO$  adducts, respectively. The  $\nu(CO)$  value gives direct information on the acid strength of the sites: the higher the  $\nu(CO)$ , the stronger is the Lewis or Brønsted acidity on the surface. Furthermore, band intensities are as a first approximation proportional to the surface density of both sites.

Over the bare  $\gamma-Al_2O_3$  (Fig. 2a), the two Lewis and Brønsted sites discussed so far, are observed. At the lowest coverage, a single band is observed at  $2194\text{ cm}^{-1}$ , due to  $Al^{3+}\cdots CO$  adducts, that progressively shifts to  $2184\text{ cm}^{-1}$ . Once the  $Al^{3+}\cdots CO$  sites reach half of their maximum intensity, a second component appears at  $2154\text{ cm}^{-1}$ , due to  $Al-OH\cdots CO$  adducts, which is not changed with increasing  $P_{CO}$ .

When the same experiment was performed on  $LaCl_3$ , KCl and liquid HCl promoted supports (La10.9, K3.1A, Cl1.4A and Cl2.8A, respectively,) activated at the same temperature, spectral changes are evident. In case of La10.9A, it is difficult to distinguish between Lewis and Brønsted sites; however, the broadening of the spectra seems to result from the contribution of both sites. Spectra obtained during the experiment on K3.1A (Fig. 2c) and Cl1.4A (Fig. 2g), show that both the intensities and the strengths of Lewis sites are decreased: moving  $\nu(CO)$  from  $2183\text{ cm}^{-1}$  to  $2181$  and  $2180\text{ cm}^{-1}$ , respectively, at the maximum CO coverage. On the other hand, the intensities and strengths of Brønsted acid sites are increased; moving  $\nu(CO)$  from  $2154\text{ cm}^{-1}$  to  $2155$  and  $2155\text{ cm}^{-1}$ , respectively. Sample K3.1A theoretically contains the same amount of Cl atoms on the surface, as that in the Cl1.4A sample. However, the decrease in Lewis sites is more remarkable on the K-promoted sample. By increasing the chlorine content on the surface (Cl2.8A), the spectra reported in Fig. 2 (h) shows that the acid strength of both sites (Lewis and Brønsted) is increased, but a very minor fraction of Lewis sites persist.

The same experiments were performed on Cu5.0, La10.9Cu5.0 and K3.1Cu5.0 catalysts, and the spectra obtained are reported in Fig. 2(d), 2(e) and 2(f), respectively. Along with the above mentioned components (Lewis and Brønsted sites), there is another band observed in the range of  $2123-2135\text{ cm}^{-1}$   $\nu(CO)$  frequency, which is due to  $Cu^+\cdots CO$  adducts<sup>10b,14</sup>. When comparison is made with the bare support (Fig. 2a), in all three cases, a minor fraction of Lewis sites persist, except in the case of K3.1Cu5.0. In addition to that, the strength of the remaining Lewis acid sites increased in the case of La10.9Cu5.0, moving  $\nu(CO)$  from  $2183$



$\text{cm}^{-1}$  to  $2189 \text{ cm}^{-1}$  at the maximum CO coverage, while it decreased in the case of K3.1Cu5.0 and Cu5.0 samples. The strength of the Brønsted acid sites increased in all three catalysts, moving the stretching frequencies of Al-OH $\cdots$ CO adducts, at high CO coverage, from  $2154 \text{ cm}^{-1}$  (unpromoted support) to 2157, 2158 and  $2163 \text{ cm}^{-1}$  on the K3.1Cu5.0, Cu5.0 and La10.9Cu5.0 catalysts, respectively. On the other hand, their population was increased on the Cu5.0 and K3.1Cu5.0 catalysts, but not on La10.9Cu5.0.

The lowest frequency bands, due to  $\text{Cu}^{+\cdots}\text{CO}$  adducts formed by the low fraction of  $\text{Cu}^+$ , were reduced during drying treatment under dynamic vacuum. From Fig. 2(d)-(f), it can be observed that the greater the strength of the Brønsted acid sites, the higher was the stretching frequency of the  $\text{Cu}^{+\cdots}\text{CO}$  adducts. The acid strength of the catalysts were in the following order: La10.9Cu5.0 > Cu5.0 > K3.1Cu5.0.

### 3.2. Catalyst screening for the ethene oxychlorination reaction

Fig. 3 shows the activity and product selectivities of various promoted catalysts for the ethene oxychlorination reaction at 503 and 573K, respectively. Fig. 3(a) shows the conversion of ethene and oxygen while Fig. 3(b) shows the selectivity to the main product 1,2-dichloroethane (1,2-EDC), as well as the by-products (mainly vinyl chloride (VCM), ethyl chloride, dichloroethane and trichloroethane). At 503 K, modest conversion was observed over all catalysts, with the unpromoted catalyst as the least active. La promoted catalyst gave the highest conversion, followed by Mg promoted and Ce,La co-promoted catalysts. At 573 K, the conversion order was altered, but the unpromoted catalyst was still the least active. K,La co-promoted catalyst gave the highest conversion, followed by Ce,La co-promoted catalyst. These two catalysts also showed the maximum selectivity to 1,2-EDC, in spite of significantly higher conversion compared to the unpromoted catalyst. In the single promoted catalyst series, La promoted catalyst showed the highest activity followed by Mg, K, Li, and Cs promoted catalysts. Concerning selectivity, K and Cs promoted catalysts showed the maximum 1,2-EDC selectivity, followed by Li, La and Mg promoted catalysts at both 503 and 573 K. From Fig. 3, it is evident that the unpromoted catalyst was less active and less selective than all promoted catalysts.

### 3.3. 1,2-EDC conversion over supports

#### 3.3.1 Screening of bare alumina, and chlorinated alumina supports

Alumina, promoted alumina supports and their chlorinated surfaces were examined for the conversion of 1,2-dichloroethane (1,2-EDC) at 503 K. From previous experience and literature data, it is known that the acidic nature and abundance of acid sites on the surface are very sensitive to the activation temperature and duration<sup>10b,15</sup>. Therefore, the experiments were performed with much care given to the activation temperature and time of activation.

Fig. 4 (a) and 4(b) show the 1,2-EDC conversion and product selectivities obtained over activated (in helium) alumina and chlorinated alumina, respectively, at 503 K during 0-135 min (0 – 60 min in the case of chlorinated alumina) of time on stream. On activated alumina, 1,2-EDC conversion was below 1% after 60 min on stream, with vinyl chloride (VCM) as the main product followed by ethyl chloride (EC), toluene and traces of 1,1-dichloroethane (1,1-EDC). There was considerable formation of higher hydrocarbons (butadiene, cyclohexane and toluene), methyl chloride ( $\text{CH}_3\text{Cl}$ ) and furan during the first 15 min on stream; however, their formation was hindered after 15 min except for toluene. From Fig. 4(b) it can be observed that remaining product selectivities were rather constant with decreasing 1,2-EDC conversion, although with a tendency of lower ethyl chloride selectivity, and higher VCM selectivity with time on stream. This observation may suggest that 1,1-EDC

is formed either from VCM or from 1,2-EDC directly, while the formation of ethyl chloride follows another route.

In addition to 1,2-EDC, the product gas may contain unconverted HCl and O<sub>2</sub>, it is therefore of interest to see how the presence of these reagent may influence the catalytic activity and selectivity of the alumina support. Upon chlorination of the alumina surface with gaseous HCl, 1,2-EDC conversion (Fig. 4 (a)) increased from less than 1 % over the activated alumina to ~10 % over the chlorinated alumina. Fig. 4(b) shows that VCM was at least 30 times more abundant over the chlorinated alumina as over non-chlorinated alumina (activated alumina). These data indicate that chlorination of alumina promoted the active sites for dehydrochlorination of 1,2-dichloroethane. Another remarkable finding is that ethyl chloride formation was completely hindered after chlorination of the alumina.

### 3.3.2 Screening of promoted alumina and chlorinated promoted alumina

It has been shown<sup>10b,16</sup> that promoters, especially potassium chloride and lanthanum chloride, significantly modify the surface acidity of alumina, as discussed in Section 3.1. La and K have further been found to have different influences on the nature and fraction of the active phase, as well as the reducibility of the oxychlorination catalyst, and thereby on its activity<sup>5a,10a,10c,d,17</sup> and selectivity<sup>5a,10b,18</sup>. For this reason, we wanted to investigate the effect of promoter chlorides (K and La) on by-product formation. The conversion of 1,2-EDC and the corresponding product yields over bare alumina and promoted alumina samples, and on their corresponding perchlorinated surfaces are reported in Fig. 5(a) and 5(b), respectively. All promoted supports gave more or less the same distribution of products, except no formation of 1,1-EDC compared to bare alumina. The main difference between the unpromoted and promoted alumina is the amount of byproducts formed. The abundance of VCM is much higher for LaCl<sub>3</sub> promoted support (almost 3 times more abundant than over bare alumina support), followed by bare alumina and KCl- promoted support. Besides VCM, ethyl chloride was formed as a second most abundant product on these supports. On the other hand, K, La co-promoted alumina gave only a negligible amount of VCM as the main product.

Upon chlorination of the surface, K and K,La promoted catalysts did not convert 1,2-EDC anymore, while bare alumina and La promoted alumina supports produced VCM as the major product. Even after chlorination, La promoted support and bare support still contained active sites responsible for formation of toluene, while it was not the case for other promoted supports. It is well known that lanthanum chloride<sup>10b,16a</sup> itself represents a strong Lewis acid-base pair, which might contribute to oligomerisation reactions.

## 3.4 1,2-EDC conversion over Cu-containing catalysts

In the final set of experiments, the activity of oxychlorination catalysts for the conversion of 1,2-EDC was examined at 503 K. Under ordinary ethene oxychlorination conditions, the catalyst contains a mixture of all active Cu phases, i.e. Cu(I)Cl, Cu(II)Cl<sub>2</sub> and Cu<sub>2</sub>OCl<sub>2</sub><sup>10a-c</sup>. In order to elucidate the effect of each of these phases on 1,2-EDC conversion, the catalysts were pretreated sequentially with ethene (Eq. (1), to form predominantly Cu(I)Cl), then O<sub>2</sub> (Eq. (2), to form predominantly Cu<sub>2</sub>OCl<sub>2</sub>) and finally with HCl (Eq. (3), to form predominantly Cu(II)Cl<sub>2</sub>), before interaction with 1,2-EDC (see Experimental section). Conversion of 1,2-EDC over Cu5.0, La10.9Cu5.0, K3.1Cu5.0 and K1.55La5.45Cu5.0 catalysts at 503 K and the corresponding product selectivities with respect to the state of the copper phase are summarized in Fig. 6 and Table 1.

### 3.4.1 Cu(I)Cl containing catalysts

During pretreatment under flowing ethene, 1,2-EDC formation was observed over all catalysts. After interaction with ethene for 30 min, it was therefore assumed that a significant fraction of copper (II) chloride was converted to copper (I) chloride, according to Eq. (1). We recently published a study showing that catalysts will experience a different degree of Cu reduction depending on the promoter added<sup>10a,10c</sup>. It was suggested<sup>10c</sup> that a La promoted catalyst was fully reduced (99%), while a K promoted catalyst had a lower degree of reduction (76%). We are not in a position to provide the quantitative fraction of Cu(I) and Cu(II) species on the surface of the catalysts studied in this work. However, the Cu phases will in all cases be shifted in the desired direction with a given pretreatment, so that a comparison is still valid.

It is observed from Fig. 6(a) and Table 1 that VCM was formed as the major product over the bare catalyst Cu5.0, with CO<sub>2</sub> and 1,1-EDC as the second and third most abundant products. Traces of ethyl chloride and 1,1,2-trichloroethane were also observed. The La promoted catalyst gave 1,1,2-trichloro ethane as the major product and VCM, CO<sub>2</sub>, 1,2-dichloroethene as minor products. On the contrary, K and K,La co-promoted catalysts did not show any activity in converting 1,2-EDC to halogenated hydrocarbons. However, a minor formation of CO<sub>2</sub> was observed, as for the other catalysts.

#### 3.4.2 Cu<sub>2</sub>OCl<sub>2</sub> containing catalysts

After the first cycle of 1,2-EDC interaction, the reactor was flushed with Ar and subsequently interacted with a stream of air for 30 min to oxidize the CuCl to copper oxychloride (Cu<sub>2</sub>OCl<sub>2</sub>), in accordance with Eq (2). Then the catalyst was subjected to 1,2-EDC stream for 60 min and the results are reported in Fig. 6(b) and Table 1. For the bare catalyst Cu5.0, CO<sub>2</sub> was formed as the major product, followed by 1,1,2-trichloro ethane and VCM. The La-promoted catalyst converted 1,2-EDC to TCE as the primary product, followed by CO<sub>2</sub>, VCM and 1,2-dichloroethene as minor products. Coming to the K promoted catalyst, a very small fraction of EDC was converted to CO<sub>2</sub> and VCM. K,La co-promoted catalyst produced TCE as the second most abundant product after CO<sub>2</sub>.

#### 3.4.3 CuCl<sub>2</sub> containing catalysts

Cu<sup>(II)</sup>Cl<sub>2</sub> species were (re)generated on the catalysts by interaction with HCl stream (Eq. (3)) for 30 min at 503 K. A 1,2-EDC feed stream was subsequently sent over the catalysts for 60 min. The respective conversion and selectivity data are reported in Fig 6(c) and the lower part of Table 1.

CuCl<sub>2</sub> species on the bare catalyst were very active in converting 1,2-EDC: It formed 1,1,2-trichloroethane and VCM as major products, followed by 1,2-dichloroethene, 1,1-EDC and CO<sub>2</sub> as minor products. The same trend was observed for the La promoted catalyst, but with higher conversion than the bare catalyst. The increase in VCM abundance is consistent with the observations made on chlorinated promoted supports (Fig. 5). But also formation of TCE and 1,2-dichloroethene increased, and this may be due to either the CuCl<sub>2</sub> phase being responsible for formation of TCE, or that modified acid sites enhanced the formation of TCE. A similar product distribution was observed over the K promoted catalysts to that of the bare and La-promoted catalysts, but in minute abundance. Finally, the K,La co-promoted catalyst gave TCE as the only product in detectable amounts.

From the above data, it is clear that Cu (II) containing species were more active for conversion of 1,2-EDC than the reduced analogue, and that their reactivity was influenced by the respective promoter added. In addition, by comparing the results obtained on the supports and Cu-catalysts, it is observed that CO<sub>2</sub> formation is more remarkable on the copper containing catalysts than on the carrier. This result suggests, not surprisingly, that the reaction

between halogenated hydrocarbons and oxygen is catalyzed by copper species rather than by acid sites of the carrier.

## 4. Discussion

### 4.1. Activity and selectivity of promoted catalysts for ethene oxychlorination catalysts

Steady state catalytic tests at 503 and 573 K for the ethene oxychlorination reaction on various promoted catalysts clearly showed that the addition of basic promoters enhanced the activity and 1,2-EDC selectivity of the catalyst. Among the single promoted catalysts, La10.9Cu5.0 catalyst showed higher conversion of ethene, followed by Mg1.9Cu5.0, K3.1Cu5.0, Li0.5Cu5.0 and CsCu5.0 and Cu5.0.

These observations are in agreement with operando XANES<sup>10a</sup>, EXAFS<sup>10b</sup>, depletive mode pulse tests<sup>10b</sup> and catalytic tests<sup>10c</sup> published previously by our team. The different capability to convert ethene and oxygen can be roughly attributed to the following characteristics: the higher activity of La10.9Cu5.0 and Mg1.9Cu5.0 is related to the ability of the promoter metal to compete with Cu(II) for the formation of an inert Cu-aluminate phase on the surface, as shown by in-situ EXAFS and XANES<sup>10c</sup>, thereby increasing the fraction of active CuCl<sub>x</sub>. A higher fraction of reducible Cu on the surface was further supported by CO-chemisorption studies<sup>10c</sup>. K3.1Cu5.0, Li0.5Cu5.0 and Cs10.4Cu5.0 catalysts showed intermediate activity. This observation was allocated to an increased fraction of active Cu species, combined with a significant formation of mixed salts with the copper species and also lesser degree of dispersion, as suggested from UV-vis, EXAFS and FTIR spectroscopy data<sup>10a,10c,18a,20</sup>, thereby modifying the activity of the copper. The observation that Li0.5Cu5.0 catalyst has higher activity than Cu5.0 can be justified by its higher fraction of active phase, as shown by in-situ EXAFS<sup>10c</sup>.

Concerning selectivity, all promoted catalysts gave higher selectivity towards 1,2-EDC than the bare Cu5.0 catalyst (Fig. 3(b)). K3.1Cu5.0 and Cs10.4Cu5.0 catalysts gave least by-product formation, which can be explained by the adverse effect of K and Cs on masking the active Lewis acid sites<sup>10b</sup>. Li0.5Cu5.0, Mg1.9Cu5.0, and La10.9Cu5.0 catalysts showed intermediate 1,2-EDC selectivity, which could be related to their higher amount of exposed Lewis acid sites<sup>10b</sup>. It has been suggested in our earlier work<sup>10b</sup> that the selectivity toward chlorinated by-products correlated directly with the density of Lewis acid sites; these results are in agreement with other literature studies<sup>5a,8b,c,19</sup>, and is a key point to understand further sections.

Interestingly, the co-promoted catalysts, K1.55La5.45Cu5.0 and Ce5.5La5.45Cu5.0, showed higher activity and 1,2-EDC selectivity compared to the single-promoted catalysts. Among these two, K1.55La5.45Cu5.0 showed the best performance, with higher conversion as well as a significant increase in the selectivity to 1,2-EDC compared with La10.9Cu5.0. Compared to K3.1Cu5.0, its activity was clearly superior, and its 1,2-EDC selectivity was very similar. It seems that the presence of K and La promoters gave a cumulative effect on the catalyst, i.e. an enhanced fraction of active Cu species due to La, combined with masking of Lewis acid sites by K. On the other hand, in the case of Ce5.5La5.45Cu5.0 catalyst, the increase in the conversion could be attributed to the ability of CeO<sub>2</sub> to act as an oxygen storage material, possibly enhancing the rate of the oxidation step (Eq. (2)), while LaCl<sub>3</sub> enhanced the rate of the reduction step (Eq. (1)) by contributing to a Cu(II)Cl<sub>2</sub> rich surface. However, it has been reported that CeO<sub>2</sub> may have a detrimental role on catalyst stability in oxychlorination reactions due to phase segregation and formation of fluorite-type phases<sup>21</sup>. Therefore, this material was not studied further.

#### 4.2. Conversion of 1,2-dichloroethane on $\gamma$ -alumina, on promoted alumina and the effect of chlorination

As mentioned in the Introduction, sequential conversion of 1,2-EDC may be an important source of byproduct formation in the oxychlorination process<sup>4a,b,5</sup>. A major target of this study was to distinguish the role of support and Cu-based phases on such sequential reactions, and elucidate to what extent they could be limited by promoter addition as well as changing reaction conditions. Concerning the role of the support, it is clear from Fig. 4 that the acidic sites of  $\gamma$ -alumina are the main active sites for conversion of 1,2-EDC to VCM, ethyl chloride and 1,1-EDC. These active acid sites even act as oligomerisation and aromatisation sites resulting in toluene formation, with quite stable activity with time on stream. This observation is in agreement with previous literature, which suggested that Lewis acid sites are responsible for dehydrochlorination reactions, while Brønsted acid sites are responsible for hydro-dechlorination reactions<sup>5c,8b,8d</sup>.

It has been shown<sup>12b,22b</sup> that by thermal activation of  $\gamma$ -alumina at and above 473 K, Al-OH sites on the surface were transformed to exposed basic sites located on a negatively charged oxygen atoms along with the transformation to unsaturated Lewis sites as shown in Scheme 2. However, their strength and population can be varied according to the chemical surroundings of the negatively charged oxygen atoms and to the thermal treatments. Further, by interaction with HCl, some of the >Al-OH groups on the alumina surface were transformed into the stronger >Al<sup>3+</sup> Lewis acid sites by interaction with HCl. HCl also increased the population of basic sites on the surface with no change in the strength of Brønsted acid sites as discussed in Section 3.1 and in other publications<sup>10b,22b,c</sup>. It has also been shown that the amount of adsorbed 1,2-EDC corresponds to the density of OH groups present on the activated alumina surface, which suggests that Brønsted sites may act as adsorption sites for 1,2-EDC molecules, thus allowing enough time for 1,2-EDC to interact with reactive sites<sup>8b</sup>.

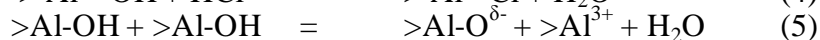
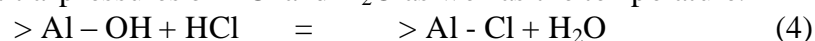
From the results of this study, we can propose that dehydrochlorination of 1,2-EDC occurred with the participation of acid-base pairs formed by the nearby Lewis acid and basic sites<sup>8b,8d</sup>, as illustrated in Scheme 3.

The data in Fig. 4(b) suggest that ethyl chloride may be formed from 1,2-EDC over the acid sites of alumina. This observation is novel compared to previous literature, which suggested that ethyl chloride is formed by direct addition of HCl to ethene<sup>5b,6a,19</sup>. There is no straightforward explanation to ethyl chloride formation without the presence of redox active sites in the absence of ethene. However, since ethyl chloride is always observed jointly with VCM, and mainly also by toluene in the product mixtures from 1,2-EDC, it is tempting to suggest that ethyl chloride is formed by a Brønsted acid catalysed hydride transfer reaction between VCM and a precursor to aromatics formation. Such hydride transfer reactions are well known from zeolite catalysis<sup>23</sup>.

As for 1,1-EDC, it has been suggested that it is formed by addition of HCl to VCM<sup>8d</sup>. Our present results are in agreement with this suggestion. From Fig. 4 (b), it can be observed that the selectivity to 1,1-EDC follows that of VCM. On a qualitative scale, it can thus be suggested that 1,1-EDC is a secondary product in the conversion of 1,2-EDC. A plausible mechanism is the formation of 1,1-EDC on the closely spaced [Cl-Al-O-Al-O-H] group, which was formed during the dehydrochlorination of 1,2-EDC, as illustrated in Scheme 3 (b), resulting in the regeneration of the former surface of alumina.

Upon exposure of the alumina surface to gaseous HCl, it has been suggested earlier<sup>10b,22b,24</sup> that HCl reacts with hydroxyls of alumina and also with Al-O-Al bridges, whereupon electron deficient aluminum atoms bind covalently to a chlorine atom by sharing one of its

non-bonding valence electron pair and form  $>Al-Cl$ ,  $Al-OH$  (and water). The processes are reversible and the relative abundance of hydroxylated versus chlorinated and dehydroxylated sites depend on the partial pressures of  $HCl$  and  $H_2O$  as well as the temperature.



In the present work, water formation ( $m/e = 18$ ) was observed when exposing the alumina surface to gaseous  $HCl$  (Fig. 1, at  $t_9$ ), whereupon our previous hypothesis about the existence of reaction (4)<sup>10b,22b,24</sup> was confirmed. Santacesaria *et al*<sup>22c</sup> have previously used thermogravimetical experiments to study reaction (4) on  $\gamma$ -alumina. The authors reported a weight increase of 2.2% in alumina after interaction with a stream of gaseous  $HCl$  at 503 K. Subsequently the sample was purged with inert gas and a weight decrease of 0.7% was reported. This means that  $HCl$  had been partially adsorbed in reversible form and partially in irreversible form. Muddada *et al*<sup>10b</sup> suggested that the regeneration of  $Al-OH$  sites upon interaction with water would be slower in this case. However, even after interaction with  $HCl$ , not all hydroxyl groups were maintained as such; some were transformed into Lewis acid-base pairs [ $=Al-O^{\delta-}$ ], cfr. Eq. (5). The IR spectra reported in Fig. 2(g) - (h) show that upon chlorination, the strength and population of Brønsted acid sites are increased as illustrated by moving  $\nu(C-O)$  in  $Al-OH \cdots CO$  adducts from 2154 to 2158-2159  $cm^{-1}$ . Furthermore, an increased Lewis acid strength was indicated by moving  $\nu(C-O)$  in  $Al^{3+} \cdots CO$  adducts from 2180 to 2202  $cm^{-1}$ .

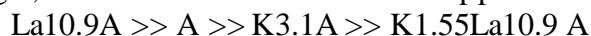
From the above experimental observations (Fig. 2g - 2h)<sup>10b</sup>, it was quite clear that, upon interaction with hydrochloric acid, acid sites of alumina (both Brønsted and Lewis) increased in strength and also formed neighboring basic [ $=Al-O^{\delta-}$ ] sites and  $Al-Cl$  groups, thereby forming acid-base pairs with increased strength. The dramatic increase in VCM formation observed after chlorination of the surface, while formation of other products was hindered, is consistent with the mechanism proposed in Scheme 3 (a). It is reasonable to suggest that most of the active Brønsted sites interacted with  $HCl$  gas molecules, thereby not participating in the formation of ethyl chloride. On the other hand, after chlorination, the newly formed [ $Cl-Al-O-Al-OH$ ] groups on the surface were active for  $HCl$  addition reaction on VCM, resulting in an increase in the formation of 1,1-EDC when compared with pure alumina (Fig. 4).

In addition to the alumina sites,  $La^{3+}$  cations themselves may act as strong Lewis sites<sup>16a</sup>, which means they can participate in the dehydrochlorination of 1,2-EDC, possibly with the help of nearby basic sites of alumina [ $=Al-O^{\delta-}$ ], forming corresponding  $>La-Cl$  and  $Al-OH$  species. It has been suggested<sup>25</sup> that lanthanum-oxide based catalysts are active in elimination of  $HCl$  from  $C_2H_5Cl$ , 1,2- $C_2H_4Cl_2$  and 1,1,2- $C_2H_3Cl_3$ . Upon chlorination of the surface with  $HCl$ , the activity increase for the  $La$ -promoted sample was significant (Fig. 5b). As for the decrease in ethyl chloride formation over the  $La$  promoted catalyst compared to the bare catalyst, one may speculate it is due to a lower abundance of Brønsted acid sites (Cfr. Fig. 2b) which are believed to be responsible for hydride transfer reactions. Formation of ethyl chloride was further hindered after chlorination. This is consistent with the observation that an increased presence of chlorine on the surface masked the active Brønsted – Lewis acid pairs. Surprisingly, formation of 1,1-EDC was completely hindered after chlorination. This observation further points to  $HCl$  as a poison for acid sites on the support surface.

On the K3.1A sample, it was shown that  $K^+$  cations were very effective in masking the Lewis acid sites, while slightly increasing the strength and abundance of Brønsted acid sites on the alumina surface. This is in accordance with the observation that the yield of ethyl chloride increased while the yield VCM decreased in relative abundance over this catalyst

compared to bare alumina (Fig. 5c vs. Fig. 5a). Upon chlorination there was no activity in converting 1,2-EDC, since the remaining active Brønsted acid sites were successfully transformed into  $>Al-Cl$ . Considering finally the co-promoted K1.55La5.45A alumina, it was very efficient in masking the sites active for 1,2-EDC conversion on alumina. From Fig. 5(d), it is observed that K,La co-promoted alumina has little activity for either dehydrochlorination, hydrochlorination or hydride transfer reactions. Upon chlorination (Fig. 5d), the support became completely inactive for either of the above reactions at 503 K.

From Fig. 5, it can be concluded that  $K^+$  and  $La^{3+}$  cations have a synergetic effect on the alumina surface and very efficiently masks both Brønsted and Lewis acid sites. The activity for converting 1,2-EDC was as follows for the supports:



#### 4.3. Conversion of 1,2-EDC on $CuCl$ / $Cu_2OCl_2$ / $CuCl_2$ species present on bare and promoted alumina

The conversion of 1,2-EDC and the relative yield of the products over Cu-containing catalysts were calculated from the results presented in Table 1 and summarised in Fig. 6. From Fig. 6(a)-(c), it is readily apparent that Cu5.0 and La10.9Cu5.0 catalysts gave higher amounts of by-product irrespective of the state of copper; while K3.1Cu5.0 and K1.55La5.45Cu5.0 catalyst gave least by-products. The main by-product formed over  $CuCl$ ,  $Cu_2OCl_2$  and  $CuCl_2$  species were VCM, trichloroethane and  $CO_2$ , while dichloroethene, 1,1-EDC and ethylchloride were formed in very small amounts.

On the copper loaded catalysts, there are still exposed acid sites on  $\gamma$ -alumina, which are the active sites in the formation of VCM, EC and 1,1-EDC. Apart from those products, TCE formation is also observed on all catalysts containing Cu(II) in the form of  $Cu_2OCl_2$  and/or  $CuCl_2$ . It is reasonable to assume that TCE is formed by chlorination of VCM. When comparing the abundance of TCE in Fig. 6(b) and 6(c), it is quite clear that TCE formation is favored on  $Cu(II)Cl_2$ , in agreement with a chlorination mechanism. Probably, all the catalysts which showed activity for TCE formation contained a certain fraction of  $Cu(II)Cl_2$ . In case of DCE formation, it was mainly observed on catalysts containing  $CuCl_2$  species, more precisely on Cu5.0 and La10.9Cu5.0. DCE is probably formed from dehydrochlorination of TCE, in analogy to VCM formation from 1,2-EDC. As concluded above, this reaction is particularly favored over bare and La promoted alumina. Quite remarkable is the formation of VCM on  $CuCl_2$  containing catalysts. This can be justified by the fact that  $CuCl_2$  was formed by interaction with gaseous HCl, which was previously shown to promote VCM formation over bare and promoted alumina. VCM formation is therefore not allocated to the  $CuCl_2$  phase, but rather to the interaction with gaseous HCl with the alumina phase.

Considering finally the formation of the most unwanted by-product, carbon dioxide, it was produced after all segments of catalyst pretreatment, however, more abundantly after interaction with air, as observed in Fig. 6(b). It can therefore be hypothesized that  $Cu_2OCl_2$  species are responsible for formation of  $CO_2$ . Besides the products formed on support, i.e. VCM, EC and 1,1-EDC; TCE, DCE and  $CO_2$  formation were hindered on K3.1Cu5.0 and K1.55La5.45Cu5.0. However, K1.55La5.45Cu5.0 catalyst gave measurable formation of TCE, irrespective of the state of the copper. This observation can be justified by the La promoter enhancing the activity of copper, in line with the high abundance of TCE formation on La10.9Cu5.0 catalysts. On the other hand, K3.1Cu5.0 catalyst gave little or no formation of TCE.

Based on the results of this study, we can propose a reaction mechanism for 1,2-EDC conversion on the catalysts with the participation of both copper chloride and acid sites on the

support, as shown in Scheme 4. First 1,2-EDC is converted to VCM on closely spaced Lewis acid-base pairs of alumina support as shown in Scheme 3. The produced VCM subsequently interacts with active copper (II) chloride sites by  $\pi$ -complexation and reacts by taking two chlorine atoms from the copper (II) chloride species as shown in Scheme 4(a) to form trichloroethane (TCE), as a parallel reaction to ethene chlorination on  $\text{Cu}^{\text{II}}$  sites. Scheme 4(b) illustrates the formation of dichloroethene (DCE) from TCE by dehydrochlorination reaction on the support sites with the participation of closely spaced basic  $[\text{>Al=O}]^-$  and  $> \text{Al-Cl}$  sites, as explained earlier in Section 4.2 and shown in Scheme 3, as a parallel reaction to VCM production from 1,2-EDC.

## 5. Conclusion

The data presented in this contribution give important leads to catalyst and process optimisation for the ethene oxychlorination reaction over  $\text{Cu}/\gamma\text{-Al}_2\text{O}_3$ -based catalysts. In particular, it was found that:

- Exposed acid sites (Brønsted and Lewis type) on the  $\gamma$  – alumina support are main sites for the conversion of 1,2-EDC to further products, thereby decreasing the 1,2-EDC selectivity during the ethene oxychlorination reaction. Catalyst promotion (with K, La, Li, Cs, Mg, or Ce) generally decreases byproduct formation
- Optimum catalyst performance was observed for K,La co-promotion, which gives superior ethene oxychlorination activity and lowers byproduct formation by increasing the fraction of active Cu species while at the same time covering Brønsted and Lewis acid sites on the support.
- Copper is more active for byproduct formation in the  $\text{Cu}(\text{II})$  state than in the  $\text{Cu}(\text{I})$  state, and this observation suggests that the ethene oxychlorination reaction should be run under reducing conditions.
- The byproduct selectivity data obtained in this contribution are generally in agreement with previously suggested reaction mechanisms. An exception is ethyl chloride formation, which has previously only been associated with ethene conversion, while it was here observed as a product of 1,2-EDC conversion.
- A summary of site – reaction correlations found in this work is given in Table 2.

## Acknowledgements

We are indebted to Dr. David Wragg and Mr. Wegard Skistad for stimulating discussions on by-product mechanisms and to Assoc. Prof. Stian Svelle and Ms. Sharmala Aravinthan for their assistance in installation of the experimental set-up. This study is part of the inGAP Center for Research-based Innovation, which receives financial support from the Norwegian Research Council under contract no. 174893.

## References

- (1) *Handbook of Heterogeneous Catalysis, 8 volumes, 2<sup>nd</sup> Edition*; 2 ed.; Ertl, G.; Knözinger, H.; Schüth, F.; and; Weitkamp, J., Eds.; Wiley -VCMH, , 2008; Vol. 1.
- (2) (a) Charles E. Wilkes; James W. Summers; Charles A. Daniels; (Eds). "*PVCM Handbook*"; Hanser Gardner Publications, Inc.: Munich, 2005(b) Nexant Chem systems; ICIS; Global Business Reports "*VCM global report*", **2009- 2012**.
- (3) (a) Cavani, F.; Teles, J. H. *ChemSusChem*, **2009**, 2, 508(b) "*Concepts of Modern Catalysis and Kinetics*"; Chorkendroff, I.; Niemantsverdriet, J. W., Eds.; Wiley - VCMH, 2007.



- (4) (a) Allen, J. A.; Clark, A. J. *Rev. Pure and Appl. Chem.*, **1971**, *21*, 145(b) Treger, Y. A.; Rozanov, V. N.; Fild, M. R.; and; Kartashov, L. M. *Russ. Chem. Rev.*, **1988**, *57*, 326(c) Mallikarjunan, M. M.; Hussain, Z. S. *J.Sci. and Ind. Res.*, **1983**, *42*, 209
- (5) (a) Arcoya, A.; Cortes, A.; Seoane, X. L. *Can. J. Chem. Eng.* **1982**, *60*, 55(b) Eichhron, H. D.; Jackh, J.; Mross, W. D.; Schuler, H.; BASF In *8<sup>th</sup> International Congress on Catalysis*, , 1985; Vol. IV-647(c) Carmello, D.; Finocchio, E.; Marsella, A.; Cremaschi, B.; Leofanti, G.; Padovan, M.; Busca, G. *J. Catal.*, **2000**, *191*, 354.
- (6) (a) Youchang, X.; Huixin, Z.; and; Ronghua, W. *Scientia Sinica*, **1980**, *23*, 979(b) "Industrial Environmental Chemistry"; Nelson, K. E.; Sawyer, D. T.; Martell, A. E., Eds.; *Plenum*: Newyork, 1992(c) NASA "'Oxidation of chlorinated hydrocarbons",'" 1995(d) Lester, G. R. *Catal. Today.*, **1999**, *53*, 407.
- (7) Maccol, A. *Chem. Rev.*, **1969**, *69*, 33.
- (8) (a) Finocchio, E.; Rossi, N.; Busca, G.; Padovan, M.; Leofanti, G.; Cermaschi, B.; Marsella, A.; Carmello, D. *J. Catal.*, **1998**, *179*, 60(b) Shalygin, A. S. *Kinet. and Catal.*, **2011**, *52*(c) Mile, B.; Ryan, T. A.; Tribbeck, T. D.; Zammitt, M. A.; Hughes, G. A. *Topics in Catal.*, **1994**, *1*, 153(d) Feijen-Jeurissen, M. M. R.; Jorna, J. J.; Neiuwenhuys, B. E.; Sinquin, G.; Petit, C.; Hindermann, J. P. *Catal. Today.*, **1999**, *54*, 65.
- (9) Avdeev, V. I.; Kovalchuk, V. I.; Zhidomirov, G. M.; d'Itri, J. L. *J. Struct. Chem.*, **2007**, *48*, S160.
- (10) (a) Muddada, N. B.; Olsbye, U.; Caccialupi, L.; Cavani, F.; Gianolio, D.; Bordiga, S.; and; Lamberti, C. *PCCP*, **2010**, *12*, 5605(b) Muddada, N. B.; Olsbye, U.; Fuglerud, T.; Vidotto, S.; Marsella, A.; Gianolio, D.; Leofanti, G.; C., L. *J. Catal.*, **2011**, *384*, 236(c) Muddada, N. B.; Olsbye, U.; Leofanti, G.; Gianolio, D.; Bonino, F.; Bordiga, S.; Fuglerud, T.; Vidotto, S.; Marsella, A.; C., L. *Dalton Trans.*, **2010**, *39*, 8437(d) Gianolio, D.; Muddada, N. B.; Olsbye, U.; Lamberti, C. *Nucl. Instr. Meth. Phys. Res. B*, **2012**, *284*, 53.
- (11) Muddada, N. B., Universitita' Delgi Studi Di Torino and Universite' De Rennes 1, 2008.
- (12) (a) Morterra, C.; Cerrato, G.; Bolis, V. *Catal. Today*, **1993**, *17*, 505(b) Morterra, C.; Magnacca, G. *Catal. Today*, **1996**, *27*, 497.
- (13) (a) Strauss, S. H. *J. Chem. Soc.-Dalton Trans.*, **2000**, 1(b) Lupinetti, A. J.; Strauss, S. H.; Frenking, G. *Prog. Inorg. Chem.*, **2001**, *49*, 1(c) Bolis, V.; Barbaglia, A.; Bordiga, S.; Lamberti, C.; Zecchina, A. *J. Phys. Chem. B*, **2004**, *108*, 9970.
- (14) (a) Lamberti, C.; Bordiga, S.; Salvalaggio, M.; Spoto, G.; Zecchina, A.; Geobaldo, F.; Vlaic, G.; Bellatreccia, M. *J. Phys. Chem. B*, **1997**, *101*, 344(b) Lamberti, C.; Palomino, G. T.; Bordiga, S.; Berlier, G.; D'Acapito, F.; Zecchina, A. *Angew. Chem. Int. Edit.*, **2000**, *39*, 2138.
- (15) (a) Leofanti, G.; Padovan, M.; Garilli, M.; Carmello, D.; Zecchina, A.; Spoto, G.; Bordiga, S.; Palomino, G. T.; Lamberti, C. *J. Catal.*, **2000**, *189*, 91(b) Leofanti, G.; Padovan, M.; Garilli, M.; Carmello, D.; Marra, G. L.; Zecchina, A.; Spoto, G.; Bordiga, S.; Lamberti, C. *J. Catal.*, **2000**, *189*, 105(c) Leofanti, G.; Marsella, A.; Cremaschi, B.; Garilli, M.; Zecchina, A.; Spoto, G.; Bordiga, S.; Fiscaro, P.; Prestipino, C.; Villain, F.; Lamberti, C. *J. Catal.*, **2002**, *205*, 375(d) Leofanti, G.; Marsella, A.; Cremaschi, B.; Garilli, M.; Zecchina, A.; Spoto, G.; Bordiga, S.; Fiscaro, P.; Berlier, G.; Prestipino, C.; Casali, G.; Lamberti, C. *J. Catal.*, **2001**, *202*, 279.

- (16) (a) Mannoilova, O. V.; Podkolzin, S. G.; Tope, B.; Lercher, J.; Stangland, E. E.; Goupil, J. M.; Weckhuysen, B. M. *J. Phys. Chem. B*, **2004**, *108*, 15770(b) Wang, S.; Borisevich, A. Y.; Rashkeev, S. N.; Glazoff, M. V.; Sohlberg, K.; Pennycook, S. J.; Pantelides, S. T. *Nature Materials*, **2004**, *3*, 143.
- (17) Sai Prasad, P. S.; Nageshwar, R. V.; Prasad, K. B. S.; Kanta Rao, P. *Solid State Ionics*, **1990**, *42*, 117.
- (18) (a) Prasad, P. S. S.; Prasad, K. B. S.; Rao, P. K.; Kaushik, V. K. *J. Mater. Sci.*, **1997**, *32*, 1479(b) Rouco, A. J. *J. Catal.*, **1995**, *157*, 380.
- (19) Marsella, A.; Carmello, D.; Finocchio, E.; Cremaschi, B.; Leofanti, G.; Padovan, M.; Busca, G. *Stud. Surf. Sci. Catal.*, **2000**, *130*, 1823.
- (20) Fontana, C. M.; Gorin, E.; Kidder, G. A.; Meredith, C. S. *Ind. Eng. Chem.*, **1952**, *44*, 363.
- (21) (a) Chao, L.; Guangdong, Z.; Liping, W.; Shuli, D.; Jing, L.; Tiexin, C. *Appl. Catal. A. General*, **2011**, *400*, 104(b) Chen, Z.; Han, M.; Wang, D.; Wei, F. *Chin. J. Catal.*, **2008**, *29*, 951.
- (22) (a) Van den Brand, J.; Snijders, P. C.; Sloof, W. G.; Terryn, H.; de Wit, J. H. W. *J. Phys. Chem. B*, **2004**, *108*, 6017(b) Digne, M.; Raybaud, P.; Sautet, P.; Guilhaume, D.; Toulhaot, H. *J. Am. Chem. Soc.*, **2008**, *130*, 11030(c) santacesaria, E.; Gelosa, D. *Ind, Eng, Chem., Prod. Res. Dev.*, **1977**, *16*, 45(d) digne, M.; Sautet, P.; Raybaud, P.; Euzen, P.; Toulhaot, H. *J. Catal.*, **2004**, *226*, 54(e) Trueba, M.; Trasatti, S. P. *Eur. J. Inorg. Chem.*, **2005**, 3393.
- (23) Cejka, J.; van Bekkum, H. (Ed.s) *Zeolites and Ordered Mesoporous Materials: Progress and Prospects*, Stud. Surf. Sci. Catal. (157) Elsevier (2005).
- (24) Zecchina, A.; Scarano, D.; Bordiga, S.; Spoto, G.; Lamberti, C. *Advances in Catalysis, Vol 51* **2001**, *46*, 265.
- (25) Alwies, W. A. M.; Van der Heijden; Mens, A. J. M.; Weckhuysen, B. M. *Catal. Lett.*, **2008**, *122*, 238.

## Figures

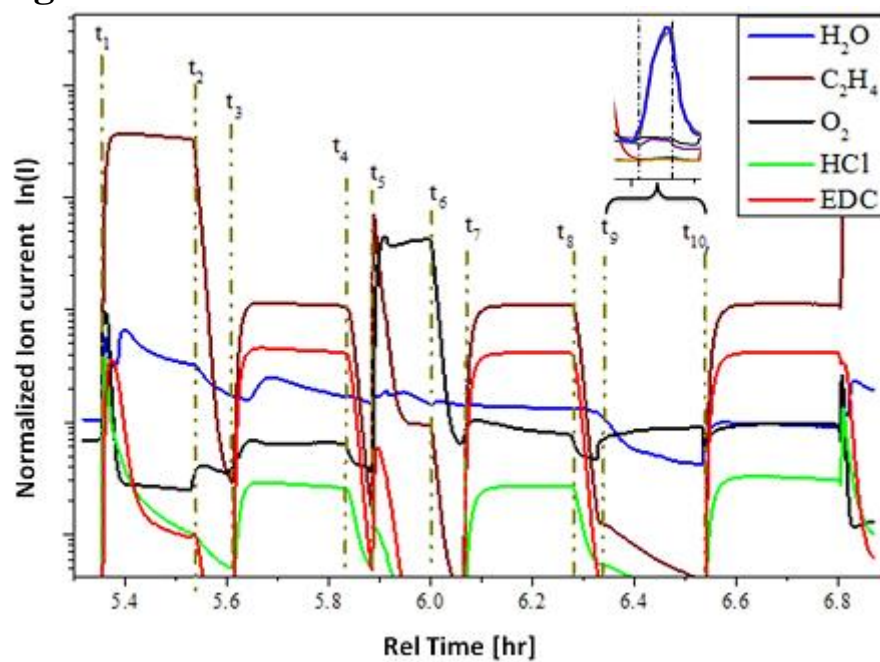


**Fig. 1:** MS signal responses of reactants and products in the reactor effluent during the operation cycle of 1,2-EDC experiments as described in Section 2.2. Inset figure is the MS signal response during HCl feed.

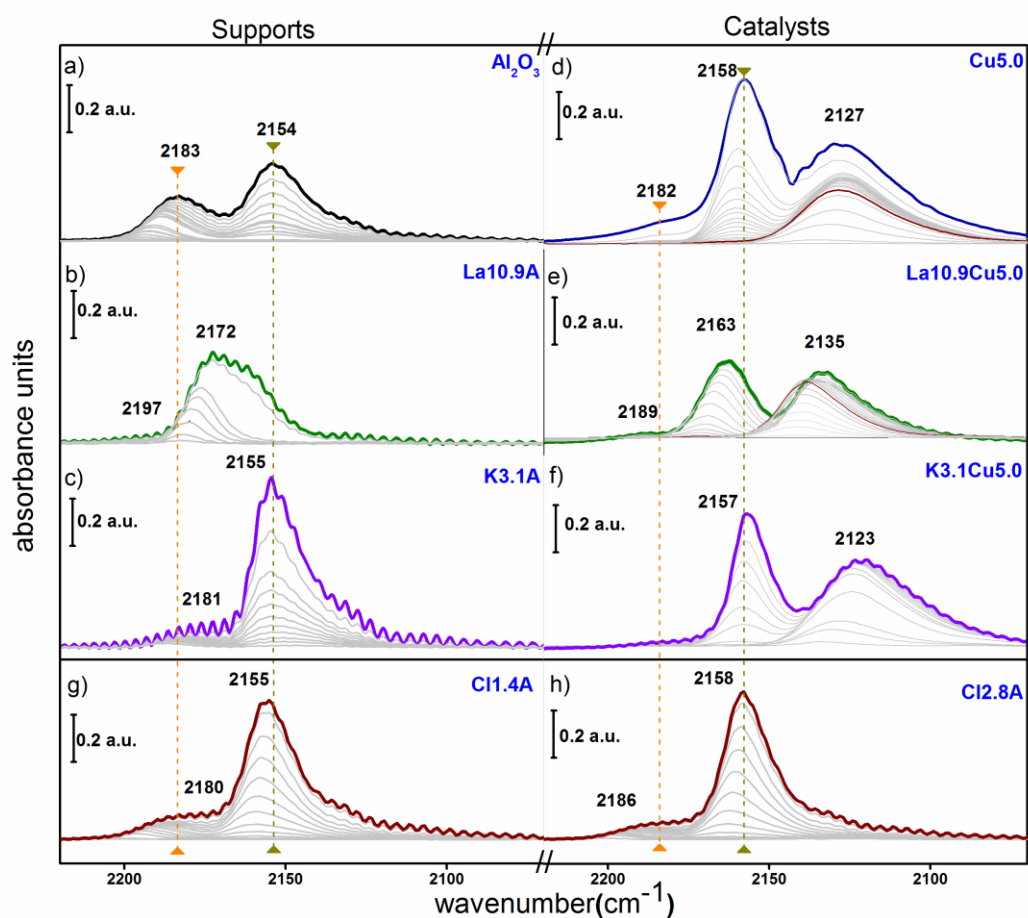


**Fig. 2:** IR spectra of CO adsorbed at liquid nitrogen temperature on supports  $\gamma\text{-Al}_2\text{O}_3$  (a), La10.9A (b), K3.1A (c); catalysts Cu5.0 (d), La10.9Cu5.0 (e), K3.1Cu5.0 (f); chlorinated samples Cl1.4A (g), Cl2.8A (h). In all cases, the samples were pre-activated at 503 K for 1 h in dynamic vacuum. (a.u. = absorbance units). This figure is composed using spectra from ref [10b].

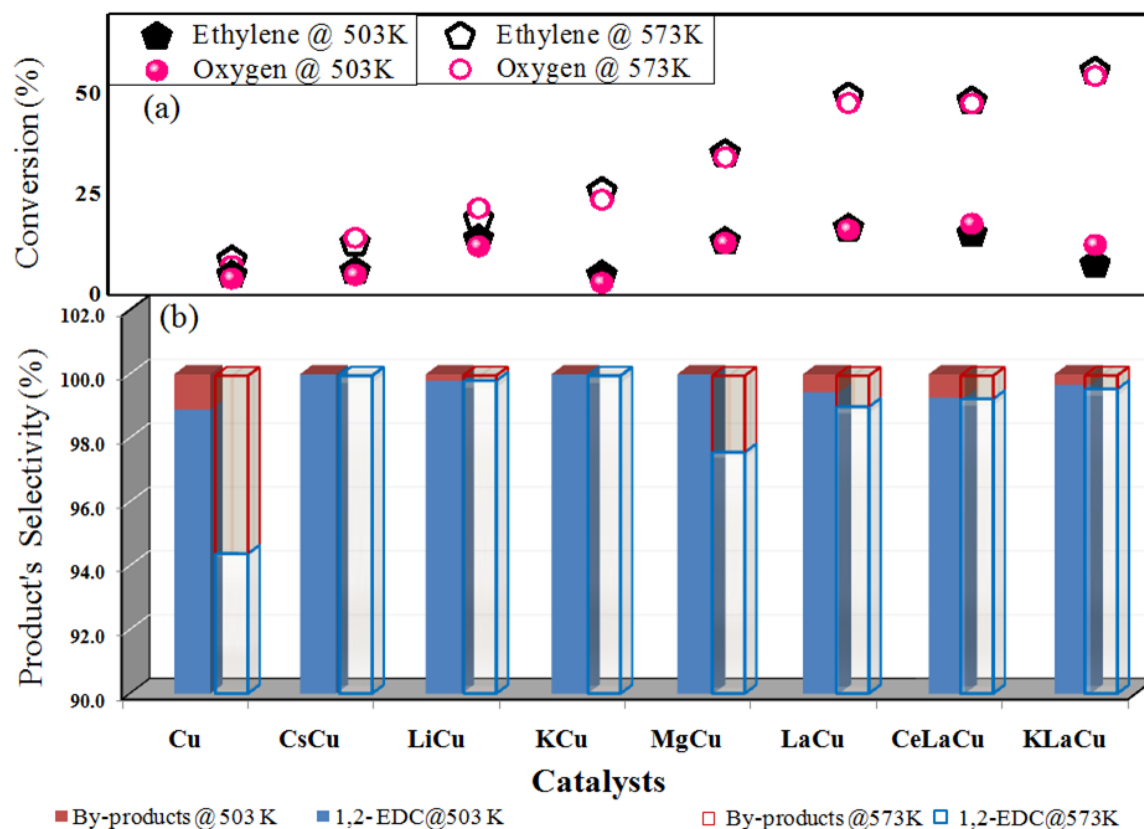


**Fig. 3:** Conversion and product selectivities obtained over Cu/ $\gamma$ -Al<sub>2</sub>O<sub>3</sub>-based catalysts in a fixed bed reactor at 503 and 573K. (a): Ethene and oxygen conversions (%). (b): Selectivities (%) to the main product 1,2 -EDC and to the by-products (VinylChloro monomer, ethyl chloride, 1,1-dichloroethane, 1,12-trichloroethane and 1,2-dichloroethene). The catalysts studied are Cu = Cu5.0, CsCu = Cs10.4Cu5.0, LiCu = Li0.9Cu5.0, KCu = K3.1Cu5.0, MgCu = Mg1.9Cu5.0, LaCu = La10.9Cu5.0, CeLaCu = Ce5.5La5.45Cu5.0 and KLaCu = K1.55La5.45Cu5.0. Open symbols represent the values obtained at 503 K and closed symbols represent the values obtained at 573 K.

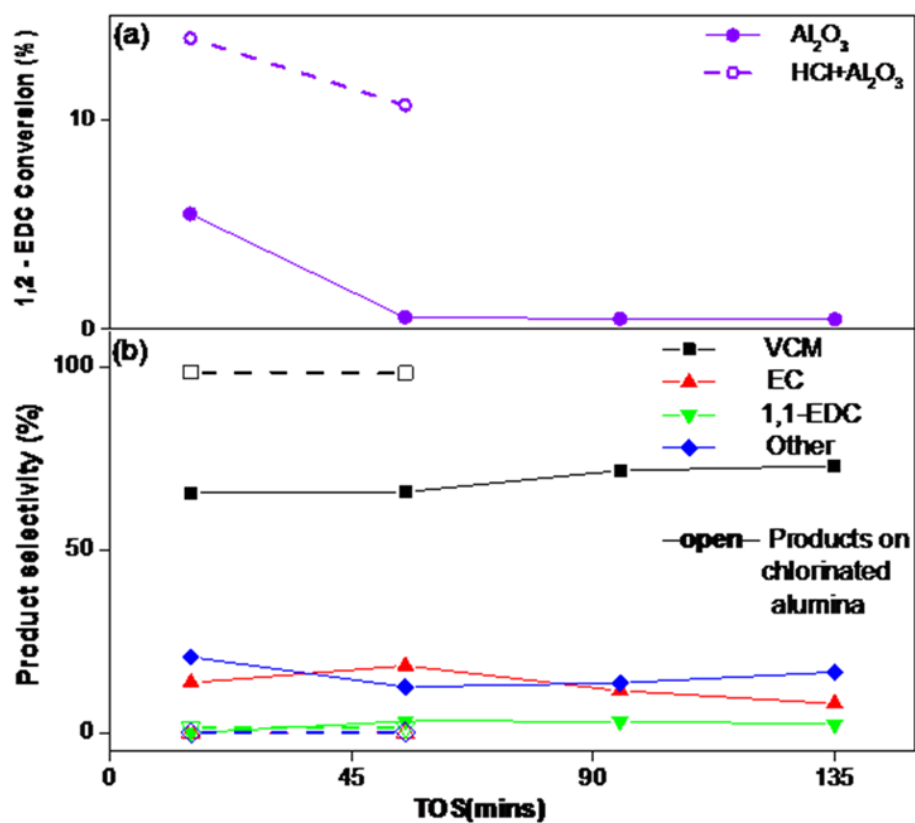


**Fig. 4:** 1,2-EDC conversion and product selectivity at 503 K plotted versus time on stream (TOS) on (a) activated alumina (closed symbols), (b) chlorinated alumina (open symbols).

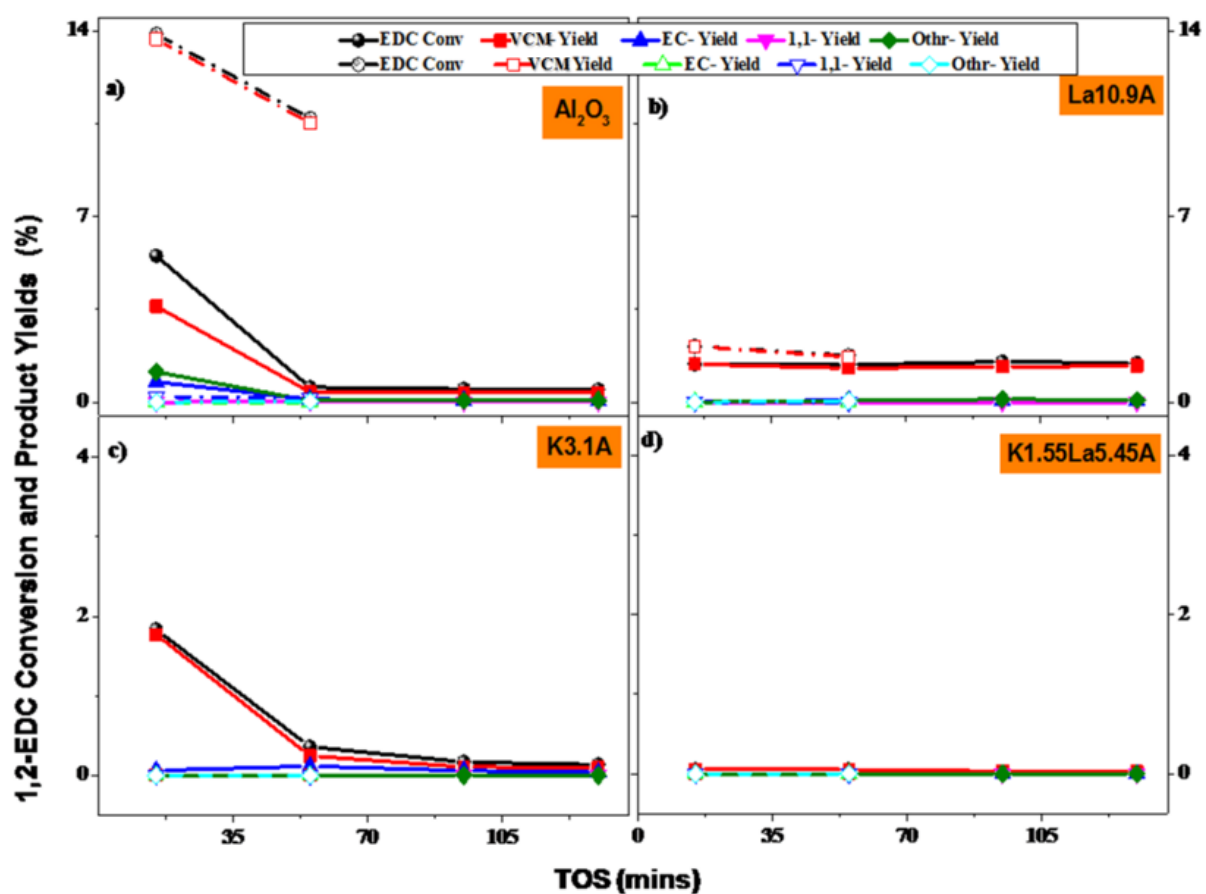
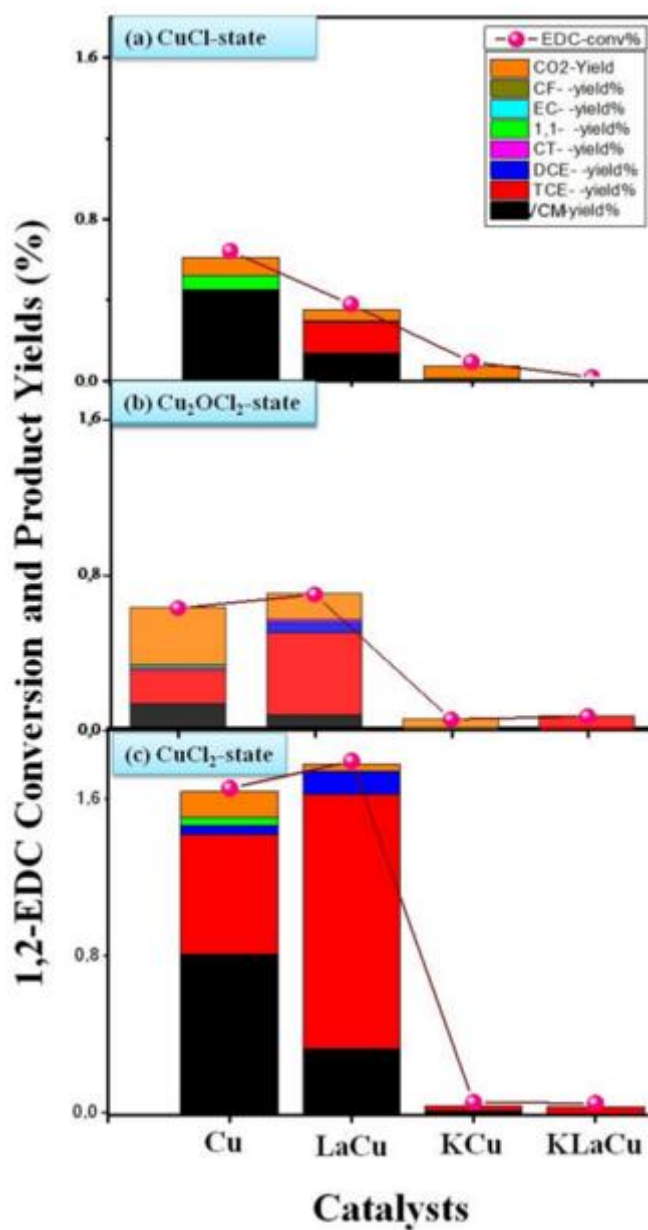


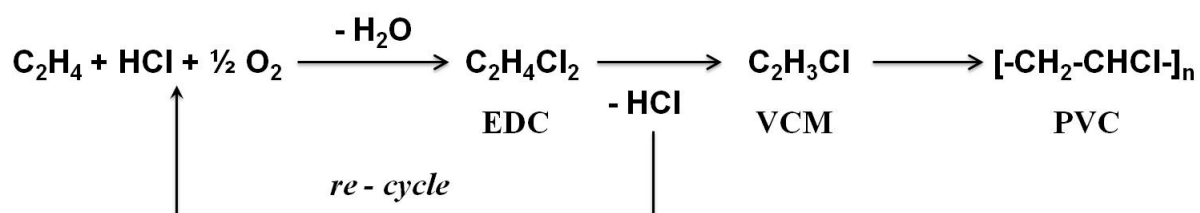
Fig. 5: Conversion of 1,2-EDC and the product selectivities at 503 K over non-chlorinated (closed symbols) and chlorinated (open symbols) supports: (a)  $\gamma\text{-Al}_2\text{O}_3$ , (b) La10.9A, (c) K3.1A and (d) K1.55La5.45A.



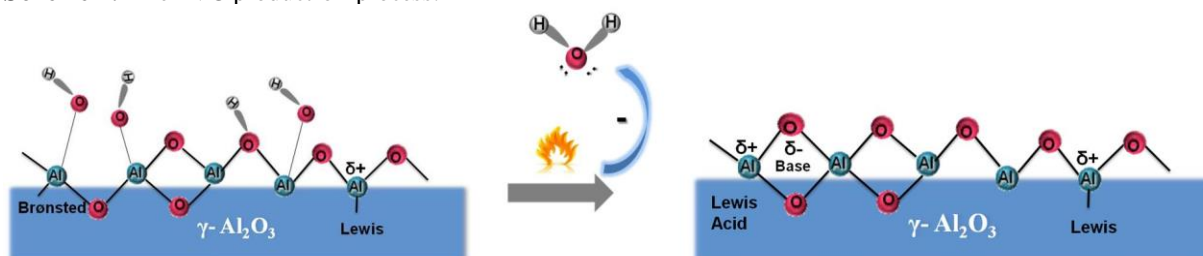
**Fig. 6:** Conversion of 1,2-EDC and product selectivities at 503 K over bare and promoted catalysts containing: (a) CuCl-rich sites, (b) Cu<sub>2</sub>OCl<sub>2</sub>-rich sites, (c) CuCl<sub>2</sub>-rich sites.

## Schemes

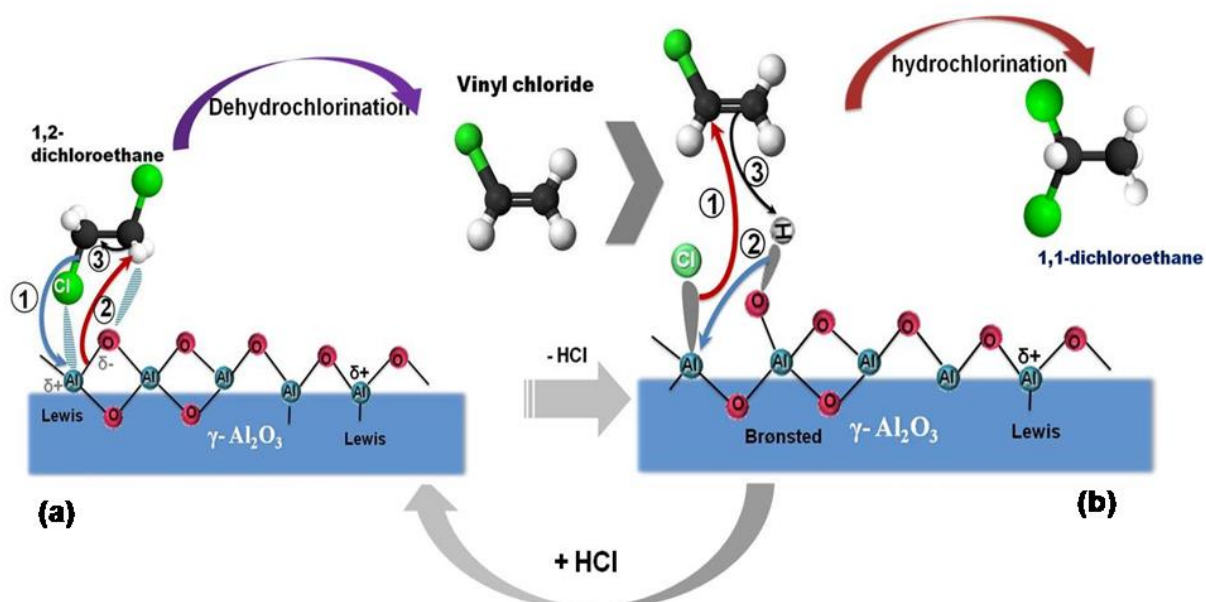




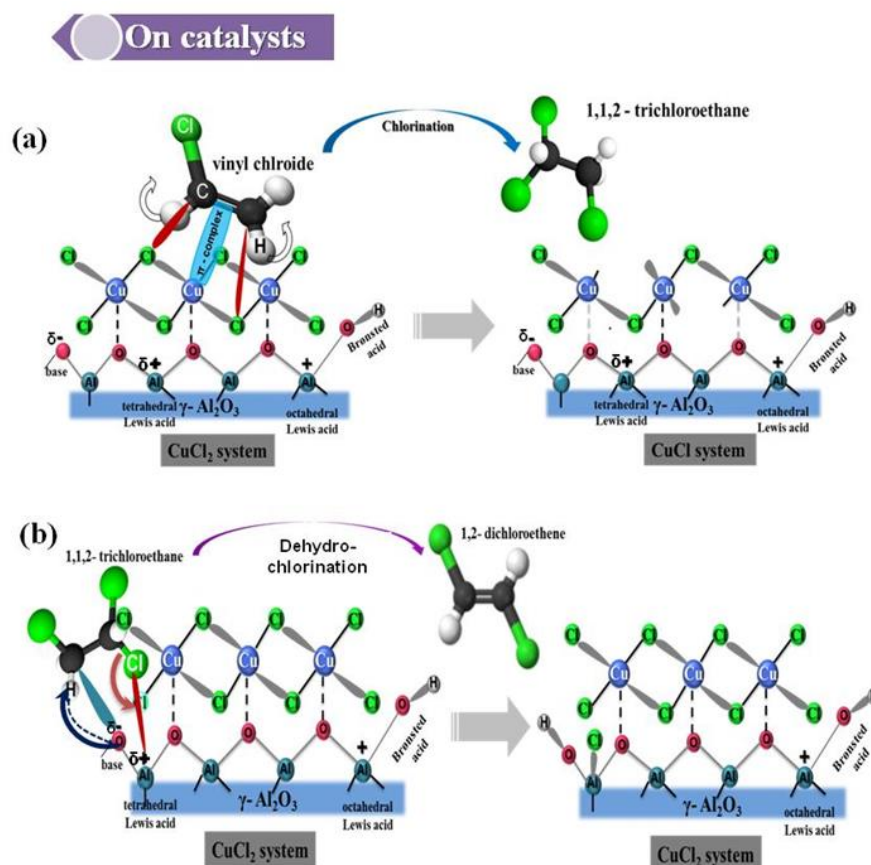
**Scheme 1:** The PVC production process.



**Scheme 2:** Schematic representation of the thermal dehydration of  $\gamma$ -alumina support.



**Scheme 3:** Schematic representation of the dehydrochlorination of 1,2-dichloroethane and subsequent hydrochlorination of vinyl chloride on modified  $\gamma$ -alumina support. Part (a) represents the thermally activated alumina, while part (b) represents the modified alumina after the dehydrochlorination reaction.



**Scheme 4:** Schematic representation of the reaction mechanism involved in the conversion of 1,2-EDC over catalysts at 503 K: (a) chlorination of VCM to form 1,1,2- trichloroethane (TCE) on  $\text{CuCl}_2$  sites of the oxychlorination catalyst; (b) subsequent dehydrochlorination of TCE to form 1,2-dichloroethene (cis /trans) on exposed support sites (Lewis acid and basic sites of alumina).

## Tables

**Table 1:** Summary of 1,2-EDC conversion (%) and corresponding product selectivities (%) at 503 K over the oxychlorination catalysts: Cu5.0, La10.9Cu5.0, K3.1Cu5.0, and K1.55La5.45Cu5.0. 1,2-EDC conversion and product selectivities are measured from the GC-MS chromatogram data acquired after 60 min of the reaction over the catalysts containing mainly one of the copper phases among CuCl, Cu<sub>2</sub>OCl<sub>2</sub> and CuCl<sub>2</sub>. “b.d.” = below detection limit

Catalyst	1,2-EDC conversion (%)	Product selectivity (%)							
		VCM	TCE	DCE	CT	1,1-EDC	EC	CF	CO <sub>2</sub>
<b>CuCl State</b>									
Cu5.0	0.6	74.1	b.d.	b.d.	b.d.	11.4	b.d.	b.d.	14.5
La10.9Cu5.0	0.4	38.9	43.5	2.1	b.d.	b.d.	b.d.	b.d.	15.5
K3.1Cu5.0	0.1	5.3	b.d.	b.d.	b.d.	b.d.	b.d.	b.d.	94.7
K1.5La5.45Cu5.0	b.d.	b.d.	b.d.	b.d.	b.d.	b.d.	b.d.	b.d.	b.d.
<b>Cu<sub>2</sub>OCl<sub>2</sub> State</b>									
Cu5.0	0.6	21.3	26.7	b.d.	2.8	2.6	b.d.	b.d.	46.5
La10.9Cu5.0	0.7	11.3	60.5	7.3	2.4	b.d.	b.d.	b.d.	18.6
K3.1Cu5.0	0.1	1.8	b.d.	b.d.	b.d.	b.d.	b.d.	b.d.	98.2
K1.5La5.45Cu5.0	0.1	b.d.	100	b.d.	b.d.	b.d.	b.d.	b.d.	b.d.
<b>CuCl<sub>2</sub> state</b>									
Cu5.0	1.5	49.6	37.3	2.6	b.d.	2.7	b.d.	b.d.	7.8
La10.9Cu5.0	1.6	18.8	72.8	6.7	b.d.	b.d.	b.d.	b.d.	1.7
K3.1Cu5.0	< 0.1	54.7	b.d.	b.d.	b.d.	b.d.	b.d.	b.d.	45.3
K1.5La5.45Cu5.0	< 0.1	b.d.	100	b.d.	b.d.	b.d.	b.d.	b.d.	b.d.

**Table 2:** Classification of the reactions and the responsible active sites involved in the conversion of 1,2-EDC over CuCl<sub>2</sub>/γ-Al<sub>2</sub>O<sub>3</sub> catalyst. LAS = Lewis acid sites, BS = Basic sites, BAS= Brønsted acid sites.

Active sites	Conversion of 1,2- EDC	
	Reaction	Products
<input type="checkbox"/> On supports > Al <sup>3+</sup> ( <b>LAS</b> ) + >Al-O <sup>(-)</sup> ( <b>BS</b> )	Dehydrochlorination	VCM, 1,2-dichloroethene (cis / trans)
>Al-Cl ( <b>LAS</b> ) + >Al-OH ( <b>BAS</b> )	Hydro-chlorination	1,1- EDC
>Al <sup>3+</sup> ( <b>LAS</b> ) + >Al-OH ( <b>BAS</b> )	Hydro-dechlorination	Ethyl chloride
<input type="checkbox"/> On supports CuCl <sub>2</sub>	Chlorination	1,1,2-trichloroethane
CuCl / Cu <sub>2</sub> OCl <sub>2</sub> / >Al-OH	Oxidation	CO <sub>x</sub>